J. Geophys. Eng. **5** (2008) 438–447 doi:10.1088/1742-2132/5/4/007

A multigrid integral equation method for large-scale models with inhomogeneous backgrounds

Masashi Endo, Martin Čuma and Michael S Zhdanov

Department of Geology and Geophysics, University of Utah, 135S 1460E, Rm 719, Salt Lake City, UT 84112, USA

E-mail: masashi.endo@utah.edu

Received 29 April 2008
Accepted for publication 23 September 2008
Published 17 October 2008
Online at stacks.iop.org/JGE/5/438

Abstract
We present a multigrid integral equation (IE) method for three-dimensional (3D) electromagnetic (EM) field computations in large-scale models with inhomogeneous background conductivity (IBC). This method combines the advantages of the iterative IBC IE method and the multigrid quasi-linear (MGQL) approximation. The new EM modelling method solves the corresponding systems of linear equations within the domains of anomalous conductivity, D_a, and inhomogeneous background conductivity, D_b, separately on coarse grids. The observed EM fields in the receivers are computed using grids with fine discretization. The developed MGQL IBC IE method can also be applied iteratively by taking into account the return effect of the anomalous field inside the domain of the background inhomogeneity D_b, and vice versa. The iterative process described above is continued until we reach the required accuracy of the EM field calculations in both domains, D_a and D_b. The method was tested for modelling the marine controlled-source electromagnetic field for complex geoelectrical structures with hydrocarbon petroleum reservoirs and a rough sea-bottom bathymetry.

Keywords: multigrid, integral equation method, large-scale, inhomogeneous background conductivity

1. Introduction

The integral equation (IE) method is one of the most important tools in three-dimensional (3D) electromagnetic (EM) modelling for geophysical applications. Over the last several years, many researchers have contributed to the improvement and development of the IE method (Xiong 1992, Hursan and Zhdanov 2002, Zhdanov 2002, Zhdanov *et al* 2006, Ueda and Zhdanov 2006). In the framework of the IE method, the conductivity distribution is divided into two parts: (1) the background conductivity, σ_b, which is used for Green's functions' calculation, and (2) the anomalous conductivity, $\Delta\sigma_a$, within the domain of integration, D. One principal advantage of the IE method over other numerical techniques, e.g. over the finite-different (FD) or the finite-element (FE) method, is that the IE method requires the discretization of the anomalous domain D only, while the FD and FE methods need a huge grid covering the entire modelling domain.

It is very well known, however, that the main limitation of the IE method is that the background conductivity model must have a simple structure to allow for an efficient Green's function calculation. The most widely used background models in EM exploration are those formed by horizontally homogeneous layers. The theory of Green's functions for layered one-dimensional (1D) models is very well developed and lays the foundation for efficient numerical algorithms. Any deviation from this 1D background model must be treated as anomalous conductivity.

In some practical applications, however, it is difficult to describe a model using horizontally layered background conductivity. For example, this situation appears in the case of geoelectrical models with bathymetry/topography and/or

 © 2008 Nanjing Institute of Geophysical Prospecting Printed in the UK

large salt dome structures present. As a result, the domain of integration may become too large, which significantly increases the size of the modelling domain and of computer memory and computational time required for IE modelling. It was demonstrated in the paper by Zhdanov *et al* (2006) that we can overcome these computational difficulties by developing the IE method with inhomogeneous background conductivity (IBC). This method is based on the separation of the effects due to excess electric current, $\mathbf{j}^{\Delta\sigma_b}$, induced in the inhomogeneous background domain, and those due to anomalous electric current, $\mathbf{j}^{\Delta\sigma_a}$, in the location of the anomalous conductivity. As a result, we arrive at a system of integral equations which uses the same simple Green's functions for the layered model, as in the original IE formulation. However, the new equations take into account the effect of the variable background conductivity distribution. The accuracy control of this method is based on application of the IBC technique iteratively.

Another challenging practical problem is related to the fact that large-scale geoelectrical models require very large computer memory and computational time for numerical calculations of the EM fields even if the IBC IE method with parallel computing is used. To overcome this problem, we have expanded the parallel IBC IE method by incorporating the principles of multigrid quasi-linear (MGQL) modelling, which was originally developed by Ueda and Zhdanov (2006) for the forward modelling on a single PC.

The new method allows us to calculate the EM fields induced in large-scale and complex geoelectrical models accurately with relatively low computational cost. We apply this new technique to study the bathymetry effects in marine controlled-source EM (MCSEM) data.

2. Integral equation formulation

In this section, for completeness, we summarize the principles of the IE method of EM modelling with inhomogeneous background conductivity (Zhdanov *et al* 2006). We consider a 3D geoelectrical model with horizontally layered (normal) conductivity σ_n, inhomogeneous background conductivity $\sigma_b = \sigma_n + \Delta\sigma_b$ within a domain D_b and anomalous conductivity $\Delta\sigma_a$ within a domain D_a (figure 1). The model is excited by an EM field generated by an arbitrary source which is time harmonic as $e^{-i\omega t}$. The EM fields in this model satisfy Maxwell's equations:

$$\begin{aligned} \nabla \times \mathbf{H} &= \sigma_n \mathbf{E} + \mathbf{j} = \sigma_n \mathbf{E} + \mathbf{j}^{\Delta\sigma_b} + \mathbf{j}^{\Delta\sigma_a} + \mathbf{j}^e, \\ \nabla \times \mathbf{E} &= i\omega\mu_0 \mathbf{H}, \end{aligned} \tag{1}$$

where

$$\mathbf{j}^{\Delta\sigma_a} = \begin{cases} \Delta\sigma_a \mathbf{E}, & \mathbf{r} \in D_a \\ 0, & \mathbf{r} \notin D_a \end{cases} \tag{2}$$

is the anomalous current within the local inhomogeneity D_a and

$$\mathbf{j}^{\Delta\sigma_b} = \begin{cases} \Delta\sigma_b \mathbf{E}, & \mathbf{r} \in D_b \\ 0, & \mathbf{r} \notin D_b \end{cases} \tag{3}$$

is the excess current within the inhomogeneous background domain D_b.

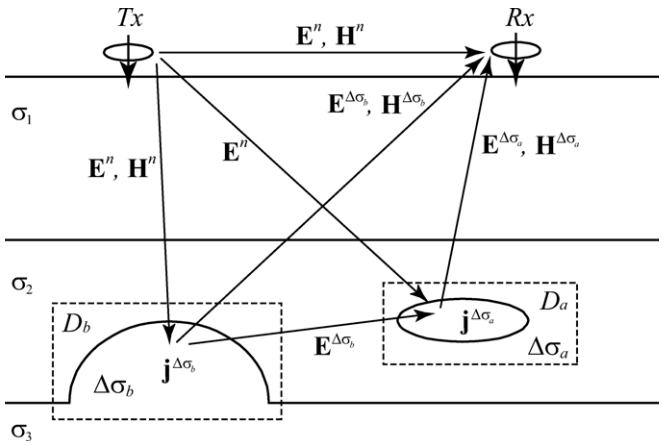

Figure 1. A sketch of a 3D geoelectrical model with horizontally layered (normal) conductivity, inhomogeneous background conductivity within a domain D_b and anomalous conductivity within a domain D_a.

Equations (1)–(3) show that one can represent the EM field in this model as a sum of the normal fields $\mathbf{E}^n$ and $\mathbf{H}^n$ generated by the given source(s) in the model with normal distribution of conductivity σ_n, variable background effects $\mathbf{E}^{\Delta\sigma_b}$ and $\mathbf{H}^{\Delta\sigma_b}$ produced by the inhomogeneous background conductivity $\Delta\sigma_b$, and the anomalous fields $\mathbf{E}^{\Delta\sigma_a}$ and $\mathbf{H}^{\Delta\sigma_a}$ related to the anomalous conductivity distribution $\Delta\sigma_a$:

$$\begin{aligned} \mathbf{E} &= \mathbf{E}^n + \mathbf{E}^{\Delta\sigma_b} + \mathbf{E}^{\Delta\sigma_a}, \\ \mathbf{H} &= \mathbf{H}^n + \mathbf{H}^{\Delta\sigma_b} + \mathbf{H}^{\Delta\sigma_a}. \end{aligned} \tag{4}$$

The total EM fields in this model can be written as

$$\mathbf{E} = \mathbf{E}^b + \mathbf{E}^{\Delta\sigma_a}, \qquad \mathbf{H} = \mathbf{H}^b + \mathbf{H}^{\Delta\sigma_a}, \tag{5}$$

where the background EM fields $\mathbf{E}^b$ and $\mathbf{H}^b$ are sums of the normal fields and those caused by the inhomogeneous background conductivity:

$$\mathbf{E}^b = \mathbf{E}^n + \mathbf{E}^{\Delta\sigma_b}, \qquad \mathbf{H}^b = \mathbf{H}^n + \mathbf{H}^{\Delta\sigma_b}. \tag{6}$$

Following the standard logic of the integral equation method (Zhdanov 2002), we write the integral representations for the EM fields of the given current distribution:

$$\mathbf{j}^{\Delta\sigma}(\mathbf{r}) = \mathbf{j}^{\Delta\sigma_b}(\mathbf{r}) + \mathbf{j}^{\Delta\sigma_a}(\mathbf{r}) = \Delta\sigma_b \mathbf{E}(\mathbf{r}) + \Delta\sigma_a \mathbf{E}(\mathbf{r}),$$

within a medium of normal conductivity σ_n:

$$\begin{aligned} \mathbf{E}(\mathbf{r}_j) &= \mathbf{E}^n + \iiint_{D_b} \widehat{\mathbf{G}}_E(\mathbf{r}_j|\mathbf{r}) \cdot \Delta\sigma_b \mathbf{E}(\mathbf{r})\, dv \\ &\quad + \iiint_{D_a} \widehat{\mathbf{G}}_E(\mathbf{r}_j|\mathbf{r}) \cdot \Delta\sigma_a \mathbf{E}(\mathbf{r})\, dv, \\ \mathbf{H}(\mathbf{r}_j) &= \mathbf{H}^n + \iiint_{D_b} \widehat{\mathbf{G}}_H(\mathbf{r}_j|\mathbf{r}) \cdot \Delta\sigma_b \mathbf{E}(\mathbf{r})\, dv \\ &\quad + \iiint_{D_a} \widehat{\mathbf{G}}_H(\mathbf{r}_j|\mathbf{r}) \cdot \Delta\sigma_a \mathbf{E}(\mathbf{r})\, dv, \end{aligned} \tag{7}$$

where the first integral terms describe the excess part of the background fields generated by the excess currents in the inhomogeneous background domain D_b:

$$\mathbf{E}^{\Delta\sigma_b}(\mathbf{r}_j) = \iiint_{D_b} \widehat{\mathbf{G}}_E(\mathbf{r}_j|\mathbf{r}) \cdot \Delta\sigma_b \mathbf{E}(\mathbf{r})\,\mathrm{d}v = \mathbf{G}_E^{D_b}(\Delta\sigma_b \mathbf{E}), \tag{8}$$

$$\mathbf{H}^{\Delta\sigma_b}(\mathbf{r}_j) = \iiint_{D_b} \widehat{\mathbf{G}}_H(\mathbf{r}_j|\mathbf{r}) \cdot \Delta\sigma_b \mathbf{E}(\mathbf{r})\,\mathrm{d}v = \mathbf{G}_H^{D_b}(\Delta\sigma_b \mathbf{E}), \tag{9}$$

and the second terms describe the anomalous fields generated by the anomalous domain D_a:

$$\mathbf{E}^{\Delta\sigma_a}(\mathbf{r}_j) = \mathbf{E}(\mathbf{r}_j) - \mathbf{E}^n(\mathbf{r}_j) - \mathbf{E}^{\Delta\sigma_b}(\mathbf{r}_j) = \iiint_{D_a} \widehat{\mathbf{G}}_E(\mathbf{r}_j|\mathbf{r}) \cdot \Delta\sigma_a \mathbf{E}(\mathbf{r})\,\mathrm{d}v = \mathbf{G}_E^{D_a}(\Delta\sigma_a \mathbf{E}), \tag{10}$$

$$\mathbf{H}^{\Delta\sigma_a}(\mathbf{r}_j) = \mathbf{H}(\mathbf{r}_j) - \mathbf{H}^n(\mathbf{r}_j) - \mathbf{H}^{\Delta\sigma_b}(\mathbf{r}_j) = \iiint_{D_a} \widehat{\mathbf{G}}_H(\mathbf{r}_j|\mathbf{r}) \cdot \Delta\sigma_a \mathbf{E}(\mathbf{r})\,\mathrm{d}v = \mathbf{G}_H^{D_a}(\Delta\sigma_a \mathbf{E}), \tag{11}$$

In equations (8)–(11), the symbols $\mathbf{G}_E^{D_{a,b}}$ and $\mathbf{G}_H^{D_{a,b}}$ denote the electric and magnetic Green's operators with a volume integration of D_a or D_b, respectively.

Using integral equations (10) and (11), EM fields at any point $\mathbf{r}_j$ can be calculated if the electric field is known within the inhomogeneity. The system of equations (10) and (11) is solved by the contraction integral equation method of Hursan and Zhdanov (2002).

The basic idea of this IE formulation is that the EM field induced in the anomalous domain by the excess currents in the background inhomogeneity $\mathbf{j}^{\Delta\sigma_b}$ can be taken into account, while the return induction effects by the anomalous currents $\mathbf{j}^{\Delta\sigma_a}$ would be ignored. In other words, the anomalous electric fields $\mathbf{E}^{\Delta\sigma_a}$ are assumed to be much smaller than the background fields $\mathbf{E}^b$ inside the domain of integration D_b in equations (8) and (9):

$$\left\| \mathbf{E} - \mathbf{G}_E^{D_b}(\Delta\sigma_b(\mathbf{E}^b + \mathbf{E}^{\Delta\sigma_a})) - \mathbf{E}^n \right\|_{D_b} \Big/ \|\mathbf{E}^b\|_{D_b} = \varepsilon_1^b \ll 1, \tag{12}$$

where $\|\cdots\|_{D_b}$ denotes the L_2 norm calculated over domain D_b:

$$\|\mathbf{E}^b\|_{D_b}^2 = \iiint_{D_b} |\mathbf{E}^b(\mathbf{r})|^2\,\mathrm{d}v,$$

and ε_1^b is the error in the background field computations.

We can also evaluate the possible errors of ignoring the return response of the currents induced in the inhomogeneous background on the field in the anomalous domain D_a:

$$\left\| \mathbf{E}^a - \mathbf{G}_E^{D_a}(\Delta\sigma_a(\mathbf{E}^a + \mathbf{E}^{\Delta\sigma_b(1)})) - \mathbf{E}^n \right\|_{D_a} \Big/ \|\mathbf{E}^a\|_{D_a} = \varepsilon_1^a, \tag{13}$$

where

$$\mathbf{E}^{\Delta\sigma_b(1)}(\mathbf{r}_j) = \mathbf{G}_E^{D_b}(\Delta\sigma_b(\mathbf{E}^b + \mathbf{E}^{\Delta\sigma_a})), \qquad \mathbf{r}_j \in D_a,$$

and

$$\mathbf{E}^a = \mathbf{E}^n + \mathbf{E}^{\Delta\sigma_a}.$$

It was demonstrated by Zhdanov *et al* (2006) that the accuracy of the IBC IE method can be improved by applying the IBC method iteratively. This means that we can take into account the return effect of the anomalous field inside the domain of the background inhomogeneity D_b and evaluate the accuracy of this solution. After that, we can use this updated background field $\mathbf{E}^{b(2)}$ in integral equation (10) for the anomalous field. The iterative process described above is continued until we reach the required accuracy of the EM field calculations in both domains D_a and D_b.

3. Multigrid QL approximation

The multigrid QL approximation, introduced by Ueda and Zhdanov (2006), is based on the following principles. A general forward EM problem is formulated in such a way that the anomalous conductivity can be treated as a perturbation from a known background (or 'normal') conductivity distribution. The solution of the EM problem in this case contains two parts: (1) the linear part, which can be interpreted as a direct scattering of the source field by the inhomogeneity without taking into account the coupling between scattering (excess) currents, and (2) the nonlinear part, which is composed of the combined effects of the anomalous conductivity and the unknown scattered field in the inhomogeneous structure. The QL approximation is based on the assumption that this last part is linearly proportional to the background field $\mathbf{E}^b$ through some electrical reflectivity vector λ (Zhdanov and Fang 1996, Gao *et al* 2004):

$$\mathbf{E}^a(\mathbf{r}) \approx \lambda(\mathbf{r})|\mathbf{E}^b(\mathbf{r})|. \tag{14}$$

In the framework of the multigrid approach, we discretize the conductivity distribution in the model and the electric fields using two grids, Σ_c and Σ_f, where Σ_c is a coarse discretization grid and Σ_f is a fine discretization grid, where each block of the original grid Σ_c is divided into additional smaller cells. First, we solve the integral equation for the electric field on a coarse grid to determine the total electric field $\mathbf{E}$. After that, we can find the anomalous field $\mathbf{E}^a$ on the coarse grid Σ_c:

$$\mathbf{E}^a(\mathbf{r}_c) = \mathbf{E}(\mathbf{r}_c) - \mathbf{E}^b(\mathbf{r}_c), \tag{15}$$

where $\mathbf{r}_c$ denotes the centres of the cells of the grid Σ_c with coarse discretization.

The components of the electrical reflectivity vector on a coarse grid are found by direct calculations as

$$\lambda_x(\mathbf{r}_c) = E_x^a(\mathbf{r}_c)/|\mathbf{E}^b(\mathbf{r}_c)|, \tag{16}$$

$$\lambda_y(\mathbf{r}_c) = E_y^a(\mathbf{r}_c)/|\mathbf{E}^b(\mathbf{r}_c)|, \tag{17}$$

$$\lambda_z(\mathbf{r}_c) = E_z^a(\mathbf{r}_c)/|\mathbf{E}^b(\mathbf{r}_c)|, \tag{18}$$

assuming that $|\mathbf{E}^b(\mathbf{r}_c)| \neq 0$.

After we have found $\lambda(\mathbf{r}_c)$, we determine the $\lambda(\mathbf{r}_f)$ values on the fine discretization grid Σ_f by linear interpolation (where $\mathbf{r}_f$ denotes the centres of the cells of the grid Σ_f with fine discretization). We compute the anomalous electric field $\mathbf{E}^a(\mathbf{r}_f)$ in the centres of the cells of the new grid Σ_f with fine discretization using expression (14):

$$\mathbf{E}^a(\mathbf{r}_f) \approx \lambda(\mathbf{r}_f)|\mathbf{E}^b(\mathbf{r}_f)|.$$

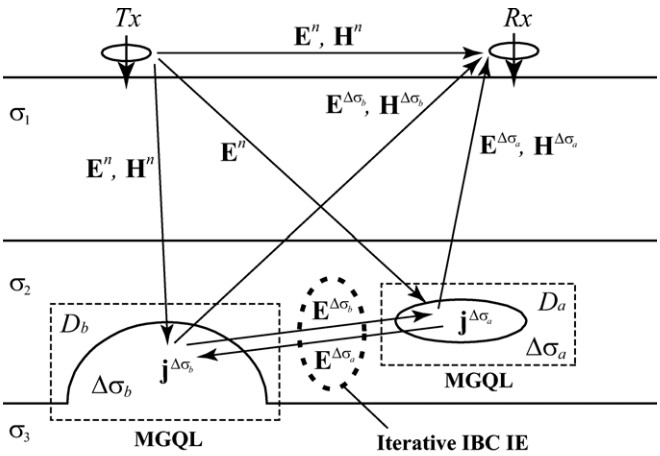

Figure 2. The concept of the MGQL iterative IBC IE forward modelling method.

We can now find the total electric field $\mathbf{E}(\mathbf{r}_\mathrm{f})$ on a new grid, as

$$\mathbf{E}(\mathbf{r}_\mathrm{f}) = \mathbf{E}^\mathrm{a}(\mathbf{r}_\mathrm{f}) + \mathbf{E}^\mathrm{b}(\mathbf{r}_\mathrm{f}). \tag{19}$$

Finally, we compute the observed fields in the receivers using the discrete analogue of the IE form of Maxwell's equations for the grid with fine discretization.

The application of the multigrid QL technique in the framework of the IBC IE method is straightforward. We introduce two pairs of coarse and fine grids, $\Sigma_\mathrm{c}^\mathrm{b}$, $\Sigma_\mathrm{f}^\mathrm{b}$ and $\Sigma_\mathrm{c}^\mathrm{b}$, $\Sigma_\mathrm{f}^\mathrm{b}$, in the inhomogeneous background, D_b, and the anomalous, D_a, domains, respectively. We solve equations (8) and (10) on the coarse grids and interpolate these solutions in the corresponding fine grids using the QL method described above. After that, we compute the observed fields in the receivers using grids with fine discretization.

Finally, the developed IBC IE forward modelling method can be summarized as follows (figure 2):

(i) EM fields in both the inhomogeneous background, D_b, and the anomalous, D_a, domains can be computed by the MGQL method,

(ii) return induction effects by the anomalous domain, D_a, on the inhomogeneous background domain, D_b, can be taken into account by the iterative IBC IE method.

4. Application of the multigrid QL IBC IE method to study the bathymetry effects in marine CSEM data

In this section we will present the application of the new method and corresponding computer code PIE3DMG, which is based on an extension of the Parallel Integral Equation PIE3D software of Yoshioka and Zhdanov (2005), for computer simulation of the bathymetry effects in the marine CSEM data. This is a very important problem in marine EM geophysics, because the effect of the sea-bottom bathymetry can significantly distort the useful EM response from a hydrocarbon (HC) reservoir, which is the main target of offshore geophysical exploration.

In order to investigate better the response of the HC reservoir, we consider first a synthetic model of a reservoir with a horizontal flat sea floor. In the second example, we present a practical case of modelling the MCSEM data in the Sabah area, Malaysia, which is characterized by extremely strong bathymetry inhomogeneities.

4.1. Model 1: a synthetic hydrocarbon reservoir

We use a typical model of the sea-bottom HC reservoir similar to that presented in Yoshioka and Zhdanov (2006). A vertical section of the geoelectrical model is shown in figure 3. One can see in this figure that a resistive structure of a hydrocarbon reservoir is located within the conductive sea-bottom sediment. The reservoir has a complex three-dimensional geometry and contains three layers: a gas-filled layer with a resistivity of 1000 Ωm, an oil-filled layer with a resistivity of 100 Ωm and a water-filled layer with a resistivity of 0.5 Ωm, as shown in figure 3. The parameters of the sea-bottom sediment are also shown in figure 3. Figure 4 presents a more detailed plan view and cross-section of the reservoir. The resistivity of the seawater layer is 0.3 Ωm and the depth of the sea floor is 1350 m below sea level.

The EM field in the model is excited by an x-directed electric horizontal bipole with a length of 270 m and located at the point with horizontal coordinates $x = 24\,000$ m and $y = 5000$ m, as shown in figure 3. The elevation of the transmitter bipole is 50 m above the sea bottom. The transmitter is assumed to generate the frequency domain EM fields at a frequency of 0.25 Hz.

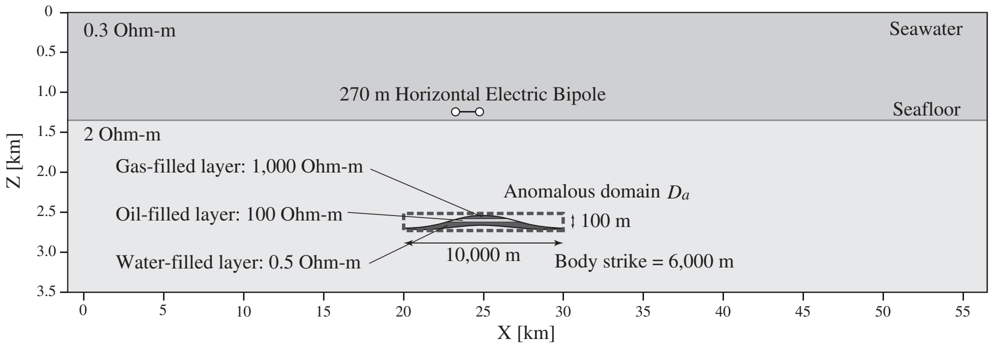

Figure 3. A model of a hydrocarbon reservoir located within a conductive sea-bottom sediment. The reservoir has a complex 3D geometry and contains three layers: a water-filled layer with a resistivity of 0.5 Ωm, a gas-filled layer with a resistivity of 1000 Ωm and an oil-filled layer with a resistivity of 100 Ωm.

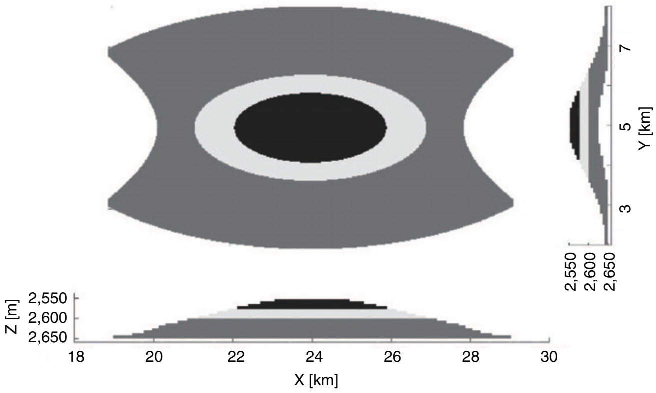

Figure 4. Detailed plan and side views of the hydrocarbon reservoir located within the conductive sea-bottom sediment.

In our numerical study, following the general principles of the IE method, the hydrocarbon reservoir structure is described by the anomalous conductivity distribution $\Delta\sigma_a$. The modelling domain D_a corresponds to the location of the reservoir, and this domain is discretized in 1.5 million cells ($400 \times 240 \times 16$) with each cell sized $25 \times 25 \times 6$ m^3 to represent accurately the reservoir structure of the model. We have applied the multigrid QL approach, which can decrease the computation cost without losing accuracy. This method first computes the EM fields on the coarse grid and then interpolates the results to the fine grid using the QL technique described above. In this case, the coarse grid has $200 \times 120 \times 8 = 192\,000$ cells. We have checked the accuracy of the multigrid approach for large-scale modelling by using this model of the HC reservoir.

Figure 5 shows amplitude plots of the in-line, E_x, and vertical electric field, E_z, as well as data for the model with a hydrocarbon reservoir obtained using the rigorous IE solution on the fine grid (line) and the MGQL approach (circles) at sea-bottom receivers located along the $y = 5000$ m line. Figure 6 shows the corresponding phase plots for the same model. One can see from these figures that the MGQL results fit the rigorous solution very accurately. At the same time, the rigorous IE solution on the fine grid using the PC cluster requires 34 min on 32 CPUs, while it takes only 6 min for MGQL modelling on four CPUs.

Figure 7 presents the plots of the total in-line, E_x, and vertical, E_z, electric fields, normalized by the amplitude of the background field along an MCSEM profile. The lines show the results obtained by the rigorous IE method using the fine grid, while the circles present the data computed using the MGQL approach. One can recognize the difference between the results of fine grid modelling and MGQL modelling; however, the maximum of the difference is less than 5%. These results demonstrate that the MGQL technique can be effectively used in large-scale EM modelling.

4.2. Model 2: Sabah area model

In this section, we apply the developed IBC IE forward modelling method to a computer simulation of a synthetic MCSEM survey in the area of Sabah, Malaysia. Sarawak Shell Berhad, Shell International Exploration and Production, and PETRONAS Managing Unit planned a SeaBed Logging™ (SBL) acquisition program to test the viability of the technology by acquiring data over geologically favourable target reservoirs in the Sabah area in 2004. They also carried out a survey for the bathymetry. We have included the detailed bathymetry data provided by Shell in this geoelectrical model. The location of the hydrocarbon reservoir was estimated from the seismic survey. We have approximately used the same location as in the real Sabah area, but we have assumed that the HC reservoir can be described by the same geoelectrical structure as in our model 1.

The EM fields in this model are generated by a horizontal electric dipole (HED) transmitter with a length of 270 m, located at the point $(x, y) = (24$ km, 5 km$)$ at a depth of 50 m above the sea bottom. The transmitter generates the EM fields with a transmitting current of 1 A at a frequency of 0.25 Hz. An array of seafloor electric receivers is located 5 m above the sea bottom along a line with the coordinates $(x = (14$ km, 34 km$)$, $y = 5$ km$)$ with a spacing of 0.2 km (figure 8).

Following the main principles of the IBC IE method, the modelling area was represented by two modelling domains,

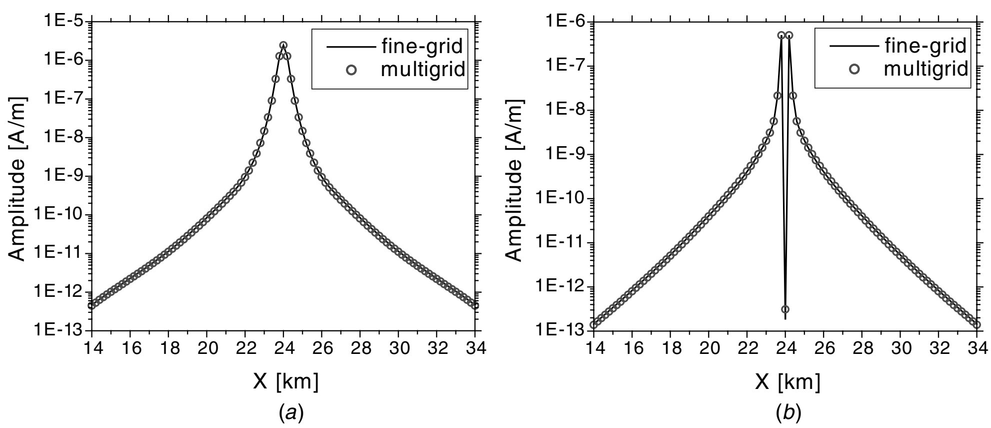

Figure 5. Amplitude plots of electric field data for the model with a hydrocarbon reservoir obtained using a fine grid (line) and a multigrid (circles). (*a*) In-line and (*b*) vertical components.

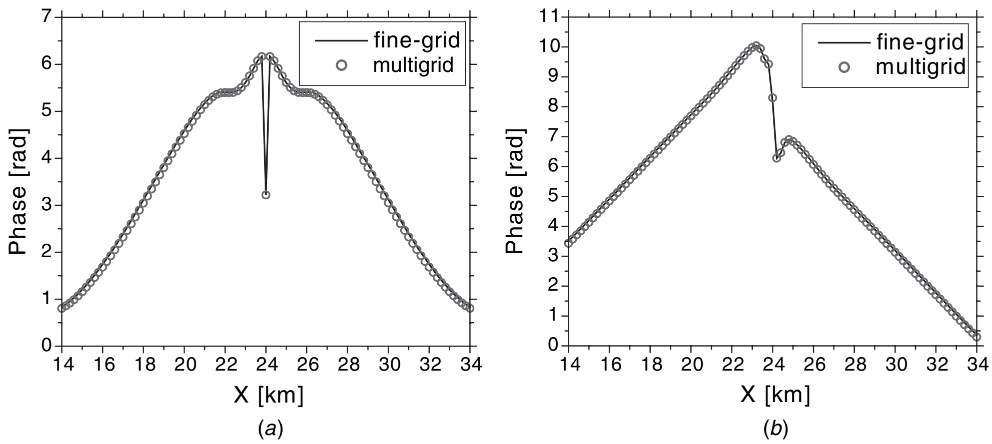

Figure 6. Phase plots of electric field data for the model with a hydrocarbon reservoir obtained using a fine grid (line) and a multigrid (circles). (*a*) In-line and (*b*) vertical components.

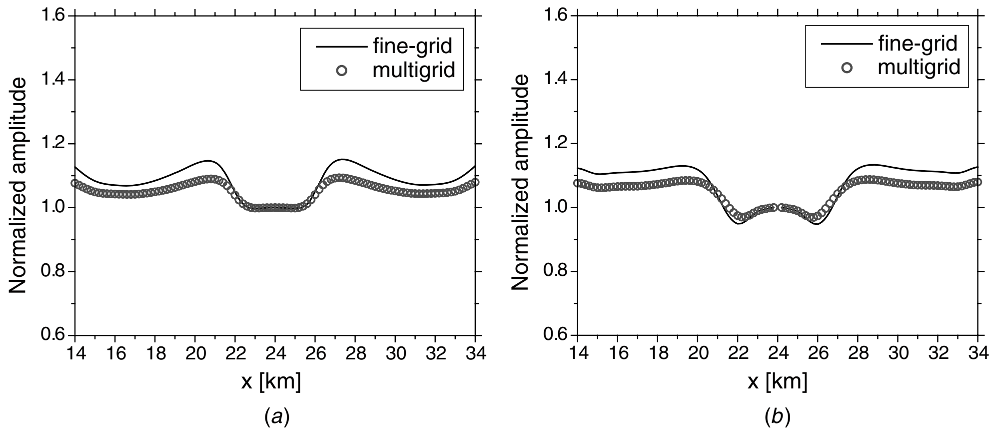

Figure 7. Plots of the total electric field, normalized by amplitude of the background field along an MCSEM profile. (*a*) In-line and (*b*) vertical components. The line shows the result obtained using a fine grid, while the circles present the data computed using a multigrid.

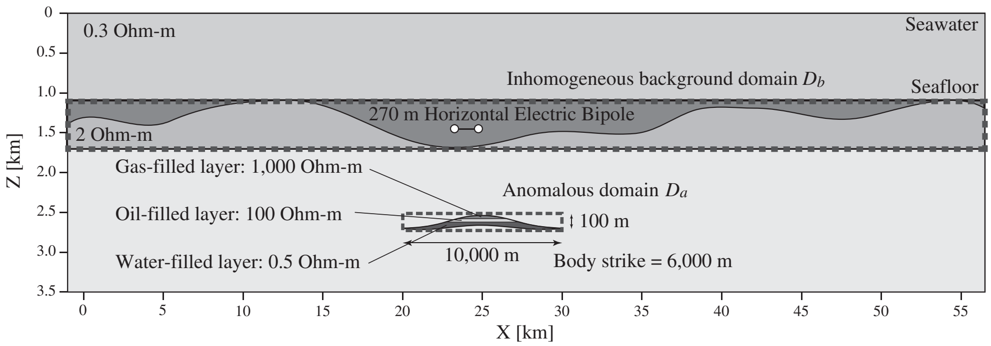

Figure 8. Sabah area model. A vertical section of a geoelectrical model of a hydrocarbon reservoir in the presence of rough seafloor bathymetry.

D_a and D_b, outlined by the dashed lines in figure 8. The modelling domain D_b covers the area with conductivity variations associated with the bathymetry of the sea bottom, while the modelling domain D_a corresponds to the location of the hydrocarbon reservoir. We used 7193 600 (1124 × 200 × 32) cells with a cell size of 50 × 50 × 20 m^3 for a discretization of the bathymetry structure. The domain D_a of the hydrocarbon reservoir area was discretized in 1536 000 (400 × 240 × 16) cells with a cell size of 25 × 25 × 6 m^3, as in model 1. A 3D relief of the bathymetry is plotted in

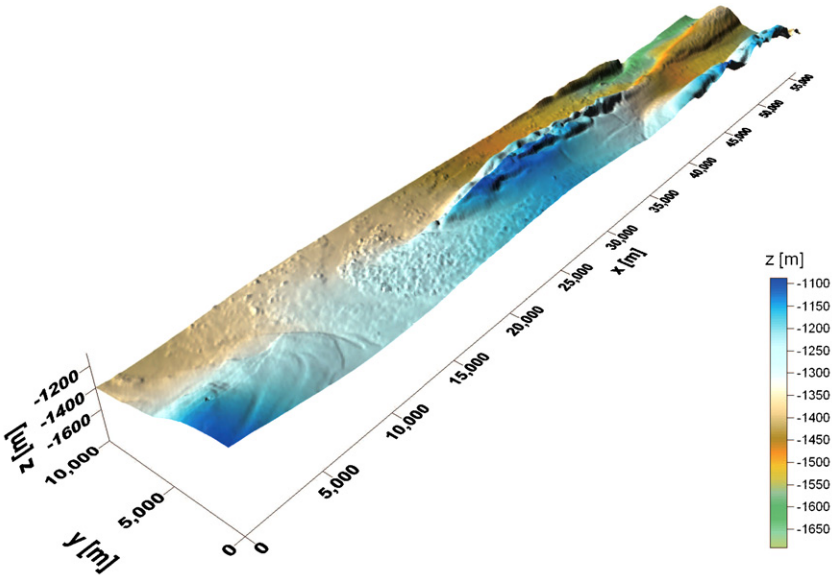

Figure 9. A 3D relief of the bathymetry for the Sabah model.

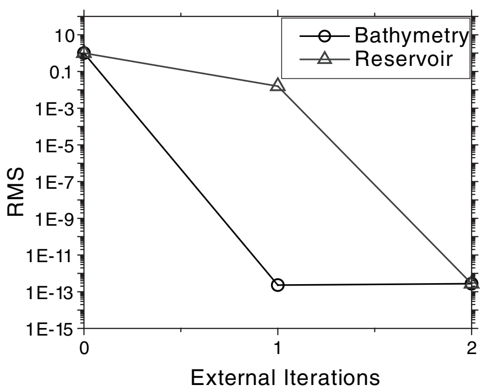

Figure 10. The convergence plot for iterative IBC IE modelling. The circles show the relative error versus the iteration number for the inhomogeneous background (bathymetry) domain, while the triangles present the same for the anomalous (reservoir) domain.

figure 9. One can see that a relatively rough bathymetry exists in the survey area.

The solution of this model by any conventional IE method would require the simultaneous solution of the corresponding system equations on a grid formed by at least a combination of two domains, D_a and D_b, which have together 8.7 million cells. At the same time, the application of the IBC IE method allows us to separate the modelling domain into two subdomains, D_a and D_b. We solve the corresponding IE of the IBC method in these domains separately, which can save a lot of computer memory and computational time. The rigorous IE solution on the fine grid using the PC cluster requires 3 h on 144 CPUs (146 GB memory and 400 GB disk space) and it takes 2 h for MGQL modelling on 24 CPUs (9.1 GB memory, 40 GB disk space). This fact results in an enormous reduction of the computing cost in interpretation of practical EM field data and also in the inverse problem solution.

We have applied the iterative version of the MGQL IBC IE method to modelling electric fields in a system of sea-bottom receivers located on a rectangular grid with a separation between the receivers of 100 m in both x and y directions. The convergence plot for iterative IBC modelling is shown in figure 10. One can see an excellent convergence rate in this figure. After just two iterations, the relative errors reach about 2.3×10^{-13} within the inhomogeneous background (bathymetry) domain and about 2.7×10^{-13} within the anomalous (reservoir) domain.

Figure 11 shows the amplitude of the total in-line, E_x, and vertical, E_z, electric fields along the MCSEM profile ($y = 5000$ m), while figure 12 presents the phase plots along the same profile, computed by the MGQL iterative IBC IE method using a fine grid (lines) and multigrid (circles). The agreements between results using a fine grid and multigrid are excellent, so that we can say that the MGQL approach is effective even for the case of an existing large inhomogeneous domain (bathymetry) by integrating this approach with the iterative technique.

Figure 13 presents the plots of the amplitude of the total in-line, E_x, and vertical, E_z, electric fields, normalized by the amplitude of the background field. The lines show the results using a fine grid, while circles represent the results using a multigrid. For the comparison, we also calculated the normalized amplitudes using a coarse grid, whose grid size is the same as that of the multigrid but no reflectivity vector is calculated during the computation. From these figures, we can recognize the effectiveness of the MGQL approach. At the same time, it is clear from these plots that the bathymetry affects the EM fields significantly. This makes it difficult to detect the reservoir by using the normalized fields calculated from the data observed in the area with rough bathymetry.

Figures 14–16, respectively, present maps of the absolute values of the x, y and z components of the total electric

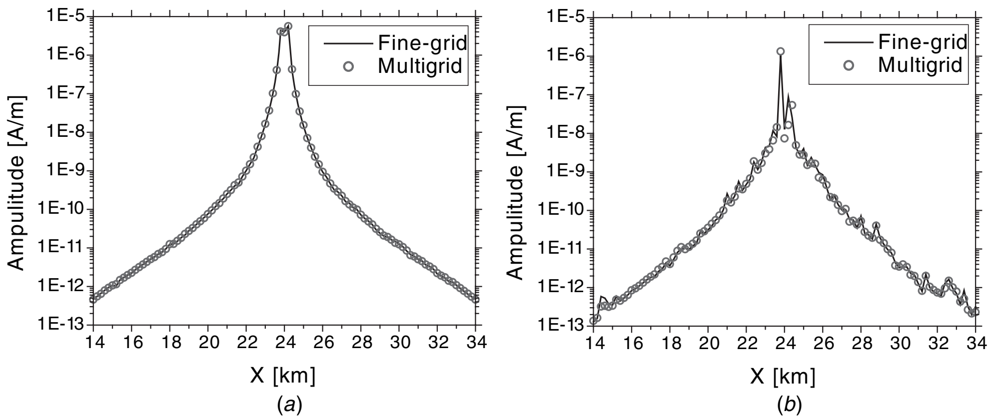

Figure 11. Amplitude plots of the observed electric field data for the Sabah area model obtained using the iterative IBC IE method. (*a*) In-line and (*b*) vertical components. The line shows the result using the fine grid, while the circles represent the result using MGQL.

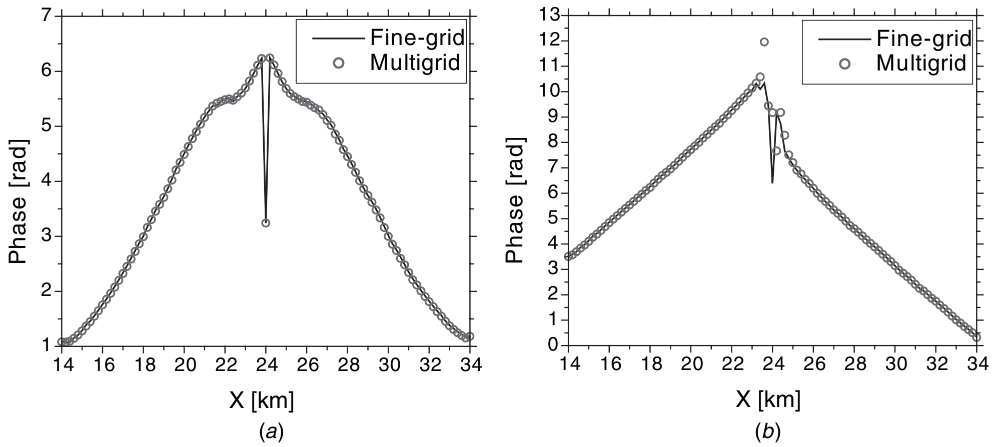

Figure 12. Phase plots of the observed electric field data for the Sabah area model obtained using the iterative IBC IE method. (*a*) In-line and (*b*) vertical components. The line shows the result using the fine grid, while the circles represent the result using MGQL.

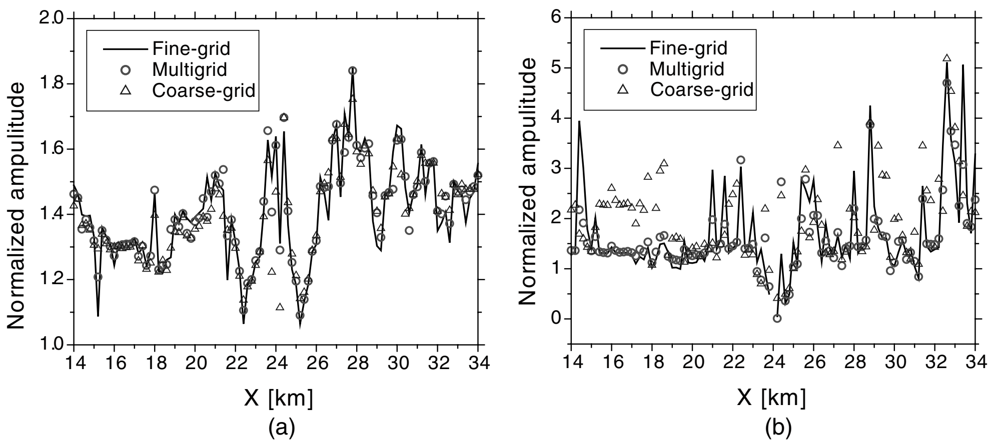

Figure 13. Plots of the total electric field, normalized by amplitude of the background field along an MCSEM profile for the Sabah area model. (*a*) In-line and (*b*) vertical components. The line shows the results using a fine grid, the circles represent the results using MGQL and the triangles indicate the result using a coarse grid.

field computed using the MGQL iterative IBC IE method. These maps also indicate that the EM fields are distorted by the bathymetry. Therefore, one should investigate the EM fields observed in the area with rough bathymetry by the modelling method which can take into account the bathymetry.

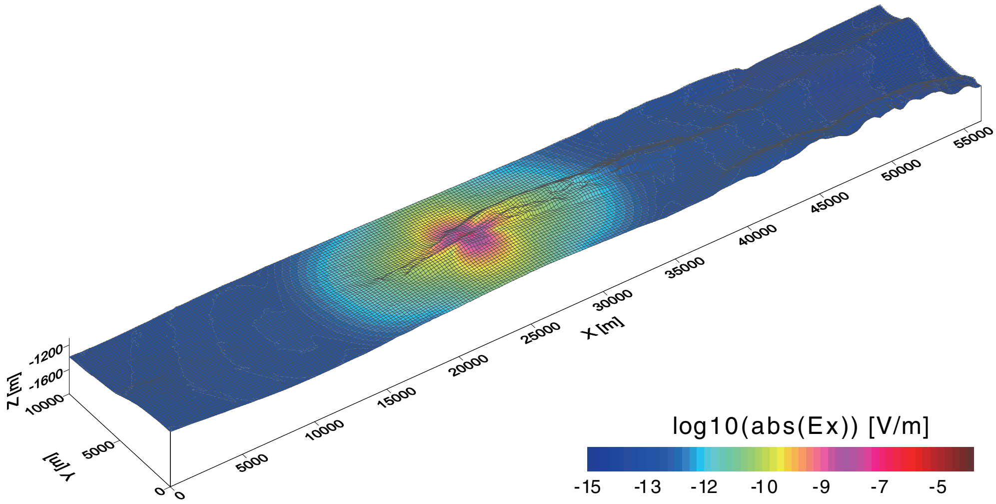

Figure 14. The map of absolute values of the x component of the electric field, computed by the MGQL iterative IBC IE method, on the sea bottom.

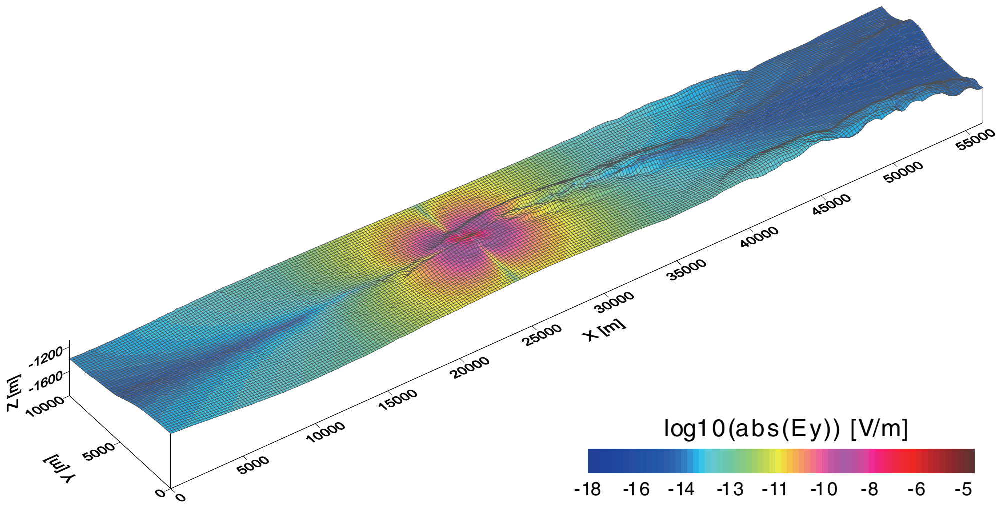

Figure 15. The map of absolute values of the y component of the electric field, computed by the MGQL iterative IBC IE method, on the sea bottom.

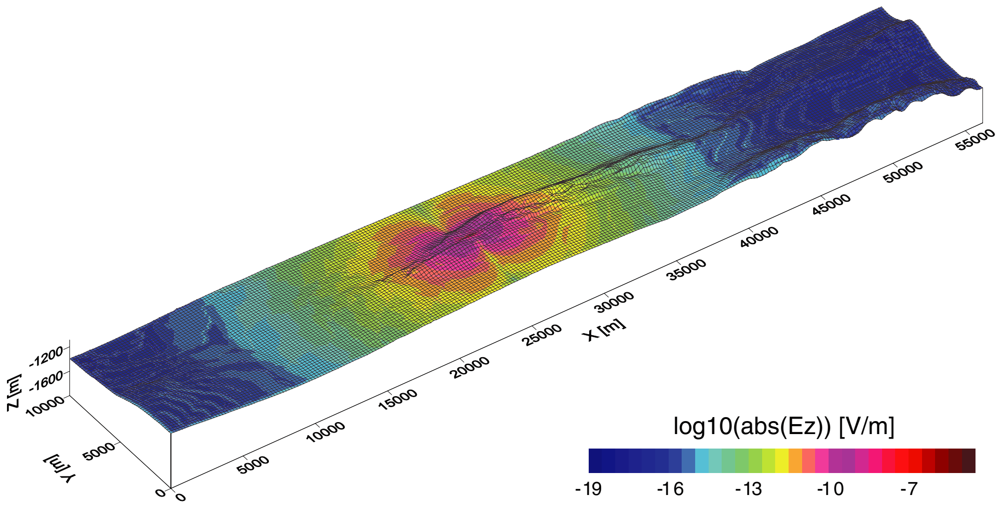

Figure 16. The map of absolute values of the z component of the electric field, computed by the MGQL iterative IBC IE method, on the sea bottom.

5. Conclusions

In this paper we have developed a new formulation of the integral equation (IE) forward modelling method, which combines together the advantages of the IE method with the inhomogeneous background conductivity (IBC) and a multigrid quasi-linear (MGQL) approximation in efficient 3D EM field computations for large-scale models. This new combined method can improve the accuracy of the solution by using iterative IBC and, at the same time, reduces the computational cost significantly by applying a multigrid approach.

We have applied a new parallel code based on the IBC IE method for modelling the MCSEM data in the area with significant bathymetric inhomogeneities. Generally, it requires a huge number of discretization cells to describe three-dimensional targets in the presence of the complex seafloor bathymetry adequately. The multigrid QL version of the IBC EM method allows us to separate this massive computational problem into at least two problems, which require a relatively smaller number of discretizations. Also, we have demonstrated that the multigrid QL approach allows us to compute the EM fields with less computational cost without losing the accuracy.

The computation results show that the EM fields can be distorted by the bathymetry (or topography). Therefore, we should use the forward modelling method which can take into account the bathymetry (or topography) for the adequate investigation of the EM data observed in the area with rough bathymetry (or topography).

Acknowledgments

The authors are thankful to Dr Mark Rosenquist of Shell for providing the Sabah area bathymetry data and permission to publish the modelling results. We also acknowledge the support of the University of Utah Consortium for Electromagnetic Modeling and Inversion (CEMI), which includes BAE Systems, Baker Atlas Logging Services, BGP China National Petroleum Corporation, BHP Billiton World Exploration Inc., BP, Centre for Integrated Petroleum Research, EMGS, ENI S.p.A., ExxonMobil Upstream Research Company, FUGRO, Halliburton, INCO Exploration, Information Systems Laboratories, Newmont Mining Co., Norsk Hydro, OHM, Petrobras, PGS, Rio Tinto-Kennecott, Rocksource, Russian Research Center Kurchatov Institute, Schlumberger, Science Applications International Co., Shell International Exploration and Production Inc., Statoil, Sumitomo Metal Mining Co. and Zonge Engineering and Research Organization.

References

Choo C L, Rosenquist M, Rollett E, Kamal A, Ghaffar A, Voon J and Wong H F 2006 Detecting hydrocarbon reservoir with seabed logging™ in deepwater, Sabah, Malaysia *SEG Expanded Abstracts* **25** 714

Gao G, Torres-Verdin C and Fang S 2004 Fast 3D modeling of borehole induction measurements in dipping and anisotropic formations using a novel approximation technique *Petrophysics* **45** 335–49

Hursán G and Zhdanov M S 2002 Contraction integral equation method in three-dimensional electromagnetic modeling *Radio Sci.* **37** 1089

Ueda T and Zhdanov M S 2006 Fast numerical modeling of multitransmitter electromagnetic data using multigrid quasi-linear approximation *IEEE Trans. Geosci. Remote Sens.* **44** 1428–34

Xiong Z 1992 Electromagnetic modeling of 3D structures by the method of system iteration using integral equations *Geophysics* **57** 1556–61

Yoshioka K and Zhdanov M S 2005 Electromagnetic forward modeling based on the integral equation method using parallel computers *SEG Expanded Abstracts* **24** 550

Yoshioka K and Zhdanov M S 2006 Modeling large-scale geoelectrical structures with inhomogeneous backgrounds using the integral equation method: application to the bathymetry effects in marine CSEM data *Proc. Annual Meeting of the Consortium for Electromagnetic Modeling and Inversion* pp 159–80

Zhdanov M S 2002 *Geophysical Inverse Theory and Regularization Problems* (Amsterdam: Elsevier) p 628

Zhdanov M S and Fang S 1996 Quasi-linear approximation in 3-D EM modeling *Geophysics* **61** 85–109

Zhdanov M S, Lee S K and Yoshioka K 2006 Integral equation method for 3D modeling of electromagnetic fields in complex structures with inhomogeneous background conductivity *Geophysics* **71** G333–45